

Developing a LRFD Procedure for Shallow Foundations

K. Lesny

Institute of Geotechnics, Department of Building Sciences, University of Duisburg-Essen, Germany

S. G. Paikowsky

Geotechnical Engineering Research Laboratory, Department of Civil and Environmental Engineering, University of Massachusetts Lowell and Geosciences Testing and Research Inc. (GTR), USA

ABSTRACT: The development of a Load and Resistance Factor Design (LRFD) procedure for the Ultimate Limit State (ULS) design of shallow foundations for highway bridges in the U.S. is presented. Large, high-quality databases of foundations on/in granular soils under varying loading conditions tested to failure are the backbone of this study. A procedural and data management framework had been developed that allowed the evaluation of the LRFD parameters. The study concentrated on the evaluation of model uncertainties associated with the bearing capacity calculation. The model uncertainties were represented by the bias defined as the ratio of measured over calculated bearing capacities using defined soil parameters and design methods. The measured bearing capacities were identified by a unique failure criterion applied to the respective load-displacement curve of the load tests. Investigation of the bearing capacity equation possible via the database identified the bearing capacity parameter N_γ to be the major source of the model uncertainty. A single resistance factor was found insufficient for addressing the bearing capacity equation. As different soil strength and loading conditions result in different levels of uncertainties, different resistance factors were required to be developed in order to maintain a consistent level of reliability under the varying conditions. The resistance factors were established on the basis of probabilistic analyses (FOSM and Monte Carlo simulations) for vertical-centric, vertical-eccentric, inclined-centric and inclined-eccentric loading conditions.

Keywords: Limit State Design, LRFD, shallow foundations, databases, uncertainty evaluation, resistance factors

1 INTRODUCTION

1.1 Methodology of LRFD and scope of the study

The intent of LRFD is to separate uncertainties in loading from uncertainties in resistance, and then to use probabilistic procedures to assure a prescribed margin of safety. In the methodology of LRFD the safety is represented by partial factors which are applied separately to the load effects and the resistance. Load effects Q_i are increased by multiplying characteristic or nominal values with load factors γ_i . The resistance is reduced by multiplying the nominal value R_n by a resistance factor $\phi \leq 1,0$. The nominal resistance results from a specific, calibrated design method and is not necessary the mean of the resistance. It then has to be ensured that the factored resistance is not smaller than a linear combination of the factored load effects:

$$\phi \cdot R_n \geq \sum_i \gamma_i \cdot Q_i \quad (1)$$

LRFD represents a Resistance Factor Approach (RFA) where the resistance factor is applied to the resulting resistance calculated with the characteristic values of the strength parameters as well as characteristic values of load components if the geotechnical resistance is defined as a function of the load effects. In opposite to the RFA the Material Factor Approach (MFA) includes the direct application of the partial factors to the characteristic values of the material, i.e. the resistance is calculated using the design values

of the material strength. Eurocode 7 (e.g. DIN EN 1997-1, 2010) generally allows both procedures in three design approaches, the member states specify in their National Annexes which design approaches finally are to be used. The RFA format in Eurocode 7 also differs slightly from the one given in equation (1) as the nominal resistance R_n is divided by a resistance factor $\gamma_R \geq 1.0$.

In the United States design specifications published by AASHTO (American Association of State Highway and Transportation Officials) are traditionally used for all federally aided highway projects and are generally viewed as the national code of highway practice. In the past two decades these specifications were gradually changed from Working Stress Design using global factors of safety (last edition of the ‘standard’ specifications are AASHTO, 1987) to LRFD within the Limit State Design (LSD) concept. While original changes mostly relied on back analysis (LSD from Working Stress Design (WSD)) and probabilistic approach, the recent development was focused on calibrations utilizing databases. In this context the NCHRP (National Cooperative Highway Research Program) research project 24-31 “LRFD Design Specifications for Shallow Foundations” was initiated with the objective to thoroughly modify Section 10 of the AASHTO LRFD Bridge Design Specifications to implement LRFD for the ULS design of shallow bridge foundations. The results of the NCHRP 24-31 research study were reported by Paikowsky et al. (2010). The major findings relevant to the bearing capacity of shallow foundations on granular soils are presented here.

1.2 Implementation procedure

The implementation of LRFD to highway bridge foundations which has been adopted in this research follows a two-step strategy:

Step 1: Assembly and assessment of knowledge and data, including:

- Defining design methods used for the calibration procedures
- Establishing databases of case histories, large and small scale model tests
- Selecting typical bridge foundation structures and case histories
- Defining expected load ranges and their distributions

Step 2: Analysis of data and methods assembled in step 1, including:

- Establishing the uncertainty of the design methods and parameters, investigation of their sources
- Developing resistance factors and their examination in design cases
- Defining final resistance factors and conditions of implementation
- Developing new design specifications

The major task within step 1 and a very important part of the research was the compilation of large, high-quality databases of foundations tested to failure. This was combined with the development of a procedural and data management framework that would enable LRFD parameter evaluation for the ULS of shallow foundations. This study is the first which introduces large-scale reliability-based design calibration of shallow foundations utilizing databases. One database includes 549 cases of field and model tests on shallow foundations in or on granular soils, predominantly subjected to vertical-centric loading, with a sizeable component of foundations subjected to combined loading. A second database provides 122 model tests of foundations on or in rock.

Different design methods for predicting the bearing capacity of shallow foundations in or on soil or rock in the ULS were compiled based on a questionnaire developed and distributed to all state bridge design agencies across the US and Canada as well as an evaluation of existing design methods based on a literature review. As a result, a set of design methods was established as the basis for the probabilistic analyses. Unique failure criteria for foundations on/in soil or rock had been defined, which were consistently used to interpret the failure loads from all load tests in the databases, thus maintaining a consistent failure interpretation for the following probabilistic analyses.

The analysis of the uncertainties associated with bearing capacity predictions was the most important task within step 2. The model uncertainties were expressed inclusively by a bias which is defined as the ratio of measured to calculated bearing resistances.

Based on the results of the uncertainty analyses for the resistances and known load uncertainties, Monte Carlo (MC) simulation as well as a simplified solution derived from First Order Second Moment (FOSM) method, have been used to determine the resistance factors for a predefined reliability index.

2 LOAD DISTRIBUTION AND LOAD FACTORS

The loads and load combinations followed those presented by AASHTO (2007) and demonstrated in examples compiled by Kimmerling (2002). In lack of better data, the uncertainty of the foundation loading has been assumed in this study as that attributed to the design of the structural element. The load factors and uncertainties for vertical live loads and dead loads on the foundation structure have been selected based on Nowak (1999) by Paikowsky et al., 2004, and are summarized in Table 1.

Table 1. Load factors and uncertainties in vertical live load and dead load

Load type	Load factor	Bias	COV
Live Load (LL)	$\gamma_L = 1.75$	1.15	0.20
Dead Load (DL)	$\gamma_L = 1.25$	1.05	0.10

The horizontal dead loads on bridge foundation structures mainly result from earth pressures due to soil and surcharge. The associated sources of uncertainty are, therefore, the variations in the soil unit weight and the soil friction angle. Live loads mainly result from impact, wind, snow, temperature variations, shrinking, creep, etc.

An analysis of the uncertainties related to lateral earth pressures suggested the load factors and uncertainties for horizontal loads as given in Table 2. A lognormal distribution is assumed with these values. The uncertainties of the dead loads are valid for a bias of the soil unit weight of 1.00 and a related COV of 0.10 for natural soil conditions and of 0.08 for engineered backfill.

Table 2. Load factors and uncertainties in horizontal live load and dead load

Load type	Load factor	Bias	COV
Live Load (LL)	$\gamma_{LFL} = 1.00$	1.00	0.15
Dead Load (DL):			
At-rest earth pressure	$\gamma_{EH0} = 1.35$	1.00	0.30
Active earth pressure	$\gamma_{EHa} = 1.50$	1.00	0.30

3 BEARING CAPACITY OF HIGHWAY BRIDGE FOUNDATIONS

3.1 Bearing capacity formulation utilized for the predicted strength limit state

The analysis was based on the procedure for the bearing capacity prediction specified in the AASHTO LRFD Bridge Design Specifications (2008). Accordingly, the general bearing capacity formulation by Vesić (1975) was used:

$$q_n = c \cdot N_{cm} + \gamma_1 \cdot D_f \cdot N_{qm} + 0.5 \cdot \gamma_2 \cdot B \cdot N_{\gamma m} \quad (2)$$

in which:

$$N_{cm} = N_c \cdot s_c \cdot d_c \cdot i_c \quad (3a)$$

$$N_{qm} = N_q \cdot s_q \cdot d_q \cdot i_q \quad (3b)$$

$$N_{\gamma m} = N_\gamma \cdot s_\gamma \cdot d_\gamma \cdot i_\gamma \quad (3c)$$

In Eq. (2) and elsewhere, c is the undrained shear strength c_u in a total stress analysis or the effective shear strength c' in an effective stress analysis. Parameters γ_1 and γ_2 are the moist or submerged unit weight of the soil above and below the footing base, respectively, whereas D_f is the embedment depth of the footing. The bearing capacity factors N_c , N_q and N_γ are summarized in Table 3, the shape factors s_c , s_q and s_γ are presented in Table 4. The depth factors d_c , d_q and d_γ , if applicable, as well as the inclination factors i_c , i_q and i_γ are given in Table 5 and Table 6, respectively.

The parameter n in Table 6 is defined as:

$$n = \left[\frac{(2 + L/B)}{(1 + L/B)} \right] \cdot \cos^2 \theta + \left[\frac{(2 + B/L)}{(1 + B/L)} \right] \cdot \sin^2 \theta \quad (4)$$

In Eq. (4) the angle θ is the angle between the resultant load and the footing length L (or L') projected in the footing area. Eq. (2) and (4) as well as Tables 4-6 are valid either for the physical footing dimensions B and L in case of centric loading or for the effective footing dimensions $B' = B - 2 \cdot e_B$ and $L' = L - 2 \cdot e_L$ in the case of eccentric loading.

The inclination factors in Table 6 and the effective footing dimensions are calculated with unfactored loads.

Table 3. Bearing capacity factors N_c (Prandtl, 1921), N_q (Reissner, 1924) and N_γ (Vesić, 1975)

Friction angle	N_c [-]	N_q [-]	N_γ [-]
$\phi_f = 0^\circ$:	$2 + \pi$	1.0	0.0
$\phi_f > 0^\circ$:	$(N_q - 1) \cdot \cot \phi_f$	$\exp(\pi \cdot \tan \phi_f) \cdot \tan^2 \left(45^\circ + \frac{\phi_f}{2} \right)$	$2 \cdot (N_q + 1) \cdot \tan \phi_f$

Table 4. Shape factors (Vesić, 1975)

Friction angle	s_c [-]	s_q [-]	s_γ [-]
$\phi_f = 0^\circ$:	$1 + 0.2 \cdot \frac{B}{L}$	1.0	1.0
$\phi_f > 0^\circ$:	$1 + \frac{B}{L} \cdot \frac{N_q}{N_c}$	$1 + \frac{B}{L} \cdot \tan \phi_f$	$1 - 0.4 \cdot \frac{B}{L}$

Table 5. Depth factors (Brinch Hansen, 1970)

Friction angle	d_c [-]	d_q [-]	d_γ [-]
$\phi_f = 0^\circ$:	$D_f \leq B: 1 + 0.4 \cdot \frac{D_f}{B}$	1.0	1.0
	$D_f > B: 1 + 0.4 \cdot \arctan \left(\frac{D_f}{B} \right)$		
$\phi_f > 0^\circ$:	$d_q - \frac{1 - d_q}{N_q - 1}$	$D_f \leq B: 1 + 2 \cdot \tan \phi_f \cdot (1 - \sin \phi_f)^2 \cdot \frac{D_f}{B}$	1.0
		$D_f > B: 1 + 2 \cdot \tan \phi_f \cdot (1 - \sin \phi_f)^2 \cdot \arctan \left(\frac{D_f}{B} \right)$	1.0

Table 6. Inclination factors (Vesić, 1975)

Friction angle	i_c [-]	i_q [-]	i_γ [-]
$\phi_f = 0^\circ$:	$1 - \frac{n \cdot H}{c \cdot B \cdot L \cdot N_c}$	1.0	1.0
$\phi_f > 0^\circ$:	$i_q - \frac{1 - i_q}{N_q - 1}$	$\left[1 - \frac{H}{V + c \cdot B \cdot L \cdot \cot \phi_f} \right]^n$	$\left[1 - \frac{H}{V + c \cdot B \cdot L \cdot \cot \phi_f} \right]^{n+1}$

3.2 Selection of soil parameters

Selected correlations were chosen in order to obtain a consistent interpretation of the soil parameters used for the bearing capacity predictions. Where SPT results were available, the soil friction angle has been correlated to the corrected SPT-N value $(N_1)_{60}$ using a procedure proposed by Peck, Hanson and Thornton as mentioned in Kulhawy & Mayne (1990):

$$\phi_f \approx 54 - 27.6034 \cdot \exp(-0.014(N_1)_{60}) \quad [^\circ] \quad (5a)$$

$$(N_1)_{60} = \sqrt{\frac{p_a}{\sigma'_v}} \cdot N_{60} \quad (5b)$$

In Eq. (5b) p_a is the atmospheric pressure, σ'_v the effective vertical stress and N_{60} the corrected SPT blow count.

For load tests conducted on medium to coarse, sharp-edged silica sand at the University of Duisburg-Essen in Germany, a correlation of the soil friction angle to the soil bulk density has been established on the basis of numerous direct shear tests. Eq. 6 is a revision of the original correlation given in Perau (1995) and was used in this study.

$$\phi_f = 3.824 \cdot \gamma - 21.527 \quad [^\circ] \quad (6)$$

where γ is in kN/m^3 .

In cases where the unit weight was not specified, but SPT results were available the soil unit weight has been correlated to the SPT blow count according to Eq. (5b) by a procedure suggested in Paikowsky et al. (1995):

$$\gamma = 0.88 \cdot (N_1)_{60} + 99 \quad [\text{pcf}] \quad \text{for } \gamma \leq 146 \text{ pcf} \quad (7)$$

4 DATABASE AND DETERMINATION OF FAILURE LOADS

4.1 Database for shallow foundations in or on soils

The UML-GTR ShalFound07 database assembled in the present research study includes 549 load tests for shallow foundations mostly in or on granular soils. The database was constructed in Microsoft ACCESS 2003. The majority of the cases are load tests to failure under vertical centric loading but a sizeable dataset of foundations under combined loading conditions is also included. Tests under vertical centric loading were either field or laboratory tests. Field tests, for which SPT blow counts were available, usually were carried out on larger foundation sizes and were categorized as tests under *natural soil conditions*. The tests under combined loading were mainly small scale laboratory model tests performed in *controlled soil conditions*. For these, the mechanical properties of the tested soils (such as unit weight, density, and shear strength) were determined in advance and were controlled in the tests; such that all the tests from one source could be compared.

The majority of the tests were carried out in Germany, USA, France and Italy. The large number of German tests originated from two sources, tests performed at the DEGEBO in Berlin (Deutsche Forschungsgesellschaft fuer Bodenmechanik) in the 1960-ies and 1970-ies and tests carried out or compiled in various research projects at the University of Duisburg-Essen during the past 25 years. Table 7 presents the content of the database classified by foundation type defined by the width of the foundation, predominant soil type below the footing base and country.

As can be seen in Table 7, there is limited number of large scale foundation tests as typically the serviceability limit is exceeded for these foundations prior to the strength limit state mobilization (i.e. bearing capacity failure). Most tests in the database are plate load tests with a width of less or equal to 1.0 m which include numerous small scale model tests under controlled laboratory conditions as mentioned above.

Table 7. Overview of cases in the UML-GTR ShalFound07 database

Foundation Type	Predominant Soil Type					Total	Country	
	Sand	Gravel	Cohesive	Mixed	Others		Germany	Others
Plate load tests, $B \leq 1$ m	346	46	--	2	72	466	253	213
Small footings, $1 \text{ m} < B \leq 3$ m	26	2	--	4	1	33	--	33
Large footings, $3 \text{ m} < B \leq 6$ m	30	--	--	1	--	31	--	31
Rafts & Mats, $B > 6$ m	13	--	--	5	1	19	1	18
Total	415	48	0	12	74	549	254	295

Note:

“Mixed” are cases with alternating layers of sand or gravel and clay or silt

“Others” are cases with either unknown soil types or with other granular materials like Loamy Scoria

The existing site conditions in the load tests were classified as shown in Figure 1. The database further includes information on the footings, the subsoil conditions, laboratory test results, field tests, details of the loading as well as the results of the load tests as load-displacement curves.

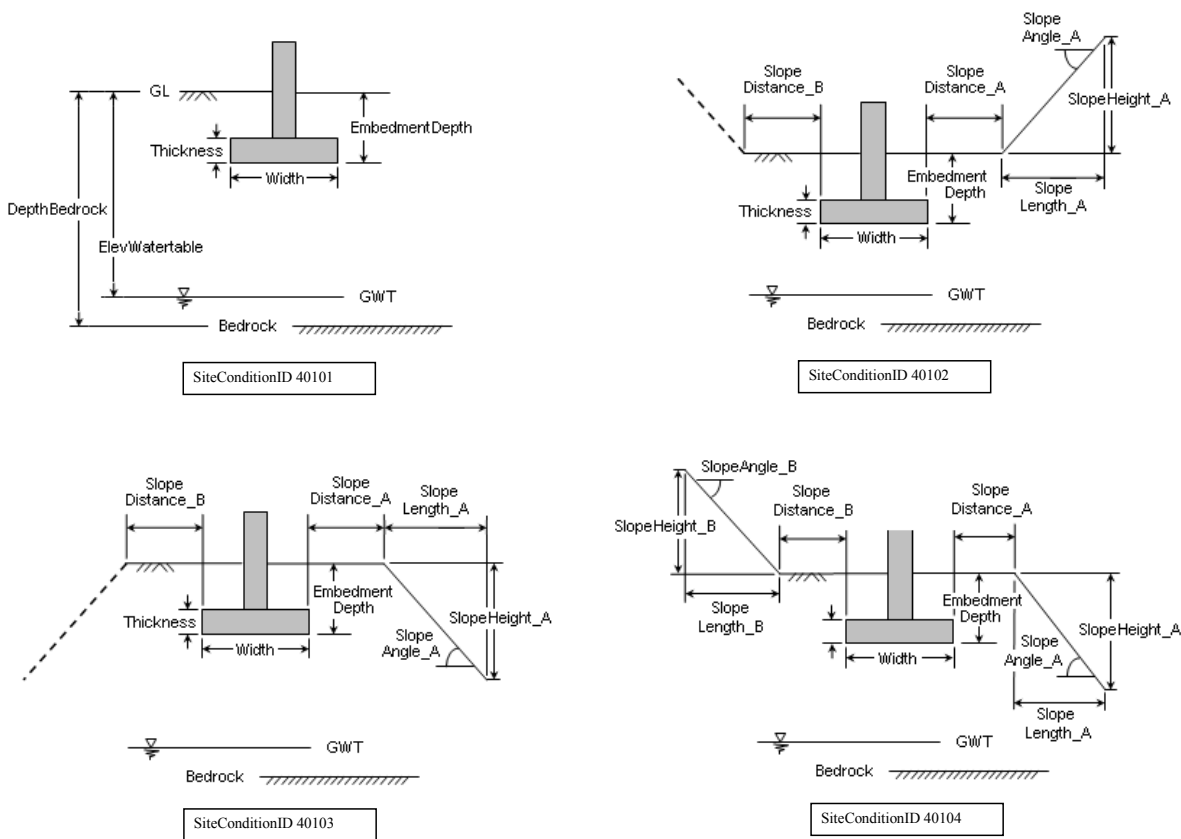


Figure 1. Classification of various site conditions employed in the UML-GTR ShalFound07 database

4.2 Failure criteria and determination of failure loads from model tests

In order to evaluate the uncertainties of the bearing capacity model provided by the formulation presented in section 3.1, a consistent procedure is required to identify the measured capacity, i.e. to define the failure loads from the load-displacement test results.

The bearing capacity equation given in Eq. (2) is valid only for a general shear failure and therefore is limited to the foundation’s relative depth of $D/B \leq 2$. In general shear, the failure pattern is completely developed and reaching the surface beside the foundation (see Figure 2). General shear failure is indicated by a distinctive peak in the load-displacement curve and can therefore be clearly identified. Usually, footings in homogenous, nearly incompressible soils with finite shear strength fail in general shear failure as shown in Figure 2. Out of the cases in the database, especially the plate load tests show this failure pattern, i.e. the small scale model tests conducted under controlled laboratory conditions where the homogeneity of the soil and its density could have been adjusted.

In field tests in inhomogeneous soils, the resultant load-displacement curves do not show a prominent peak indicating a general shear bearing capacity failure. For non-dense soils, the foundation fails in local or punching shear. Depending on the actual mode of failure, a clear peak or at least an asymptote value may not exist at all, so that the failure load needs to be interpreted. Such interpretation requires a load test to be conducted to sufficiently large displacements. Large scale field tests were typically performed to limited displacements where a bearing capacity failure could not be developed or identified. This led to a reduction in the number of load tests available for the reliability analyses.

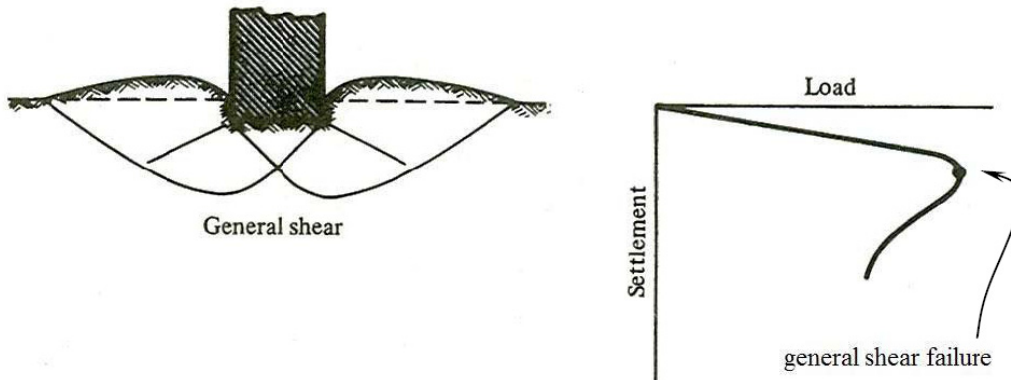


Figure 2. Bearing capacity failure as a general shear failure (Vesić, 1975)

The following criteria for interpreting the failure loads from load-displacement curves have been investigated in this study:

- Minimum slope criterion (Vesić, 1963)
- Limited settlement criterion (Vesić, 1975)
- Interpretation from the log-log plot of the load-displacement curve (De Beer, 1967)
- Two slope criterion (e.g. NAVFAC, 1986)

With the minimum slope criterion (Vesić, 1963) the failure load is defined at the point where the slope of the load-displacement curve first reaches zero or a minimum steady value. For footings in or on soils with high relative density which are more likely to fail in general shear failure the starting point of the minimum slope usually is clearly defined. For footings in or on soils with lower densities the definition of the failure load may sometimes be arbitrary. In this case, a semi-log scale with the load in logarithmic scale may help to identify the failure load.

The limited settlement criterion introduced by Vesić (1975) includes the definition of the failure load at a limited settlement of 10% of the footing width.

If the load-displacement curve is presented in a logarithmic scale with loads and displacements either as normalized or as absolute values, the failure load can be interpreted as the point of break in the load-displacement curve (De Beer, 1967).

The two slope criterion (e.g. NAVFAC, 1986) is a variation of the minimum slope criterion or De Beer's criterion and can be applied by constructing the asymptotes at the initial portion as well as at the end portion of the load-displacement curve which is plotted either in a linear or a logarithmic scale. The load at the intersection point of both asymptotes represents the failure load. A range of failure load may be identified if the location of the end asymptote is not unique.

The application of these failure criteria to the UML-GTR ShalFound07 database was examined for the tests on vertical-centric loading. Out of these tests, 196 cases could have been interpreted using the minimum slope criterion and 119 using De Beer's criterion based on the log-log plot of the load-displacement curves. Most of the footings, especially in small scale model tests on very dense soils, failed before reaching a settlement of 10% of the footing width. This criterion could therefore only be applied to 19 cases.

In order to examine and compare the failure criteria and to establish the uncertainty of the criterion selected for defining the bearing capacity of shallow foundations on soils, a single "representative" value of the relevant measured capacity was assigned to each footing case. This was done by taking an average of the measured capacities interpreted using the minimum slope criterion, the limited settlement criterion of 0.1B (Vesić, 1975), the log-log failure criterion, and the two-slope criterion (shape of curve). The values obtained by each of the failure criteria were then compared case by case to the representative value. The statistics of the ratios of this representative value over the interpreted capacity using the minimum slope criterion and the log-log failure criterion were comparable with the mean of the ratio for the minimum

slope criterion being 0.98 versus that for the limited settlement criterion being 0.99. Due to the simplicity and versatility of its application, the minimum slope criterion was selected as the failure interpretation criterion to be used for all cases of footing, including those with combined loadings. Figure 3 shows the histogram for the ratio of the representative measured capacity to the interpreted capacity using the minimum slope criterion. Figure 3 represents, therefore, the uncertainty associated with the use of the selected criterion, suggesting that the measured capacity interpreted using the minimum slope criterion has a slight overprediction.

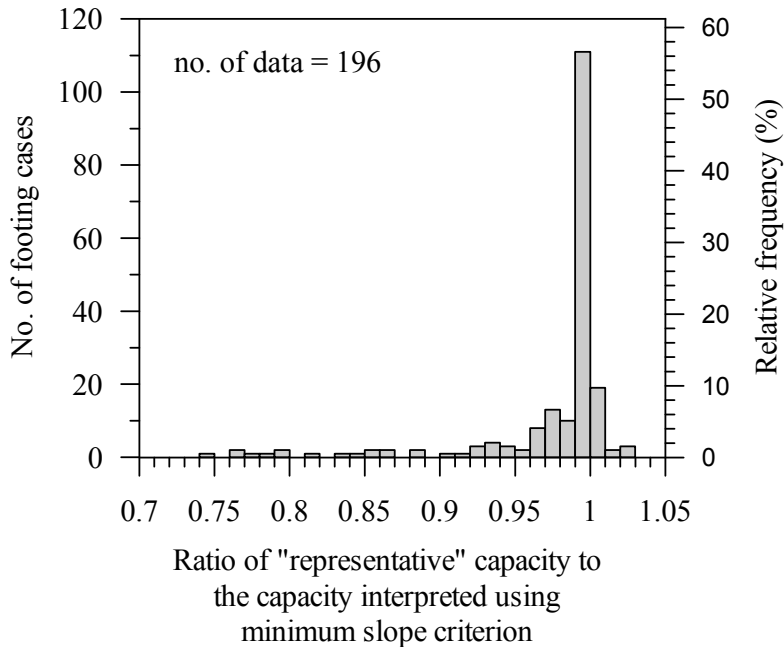


Figure 3. Histogram for the ratio of representative measured capacity to interpreted capacity using the minimum slope criterion for 196 footing cases in granular soils under vertical-centric loading.

5 EVALUATION OF MODEL UNCERTAINTIES

5.1 Definition of the bias

The uncertainty of the geotechnical resistance model controls the resistance evaluation of the foundation due to the assumptions and empirical data utilized in its formulation. To evaluate the model uncertainty the bearing capacity model presented in section 2.2 was calibrated as a complete unit while other associated sources of uncertainty were reduced by applying specific procedures, e.g. the soil parameter establishment as previously discussed. This approach, while may be in dispute, was proven effective when applied to the design of deep foundations (see example in Paikowsky et al., 2010) or when examined theoretically against a case study (Teixeira et al., 2011).

The uncertainty associated with the bearing capacity calculation was evaluated on the basis of the test results in the databases by comparing the bearing capacities measured in the load tests with the calculated bearing capacities using the calculation methods defined in section 2.2. The ratio of measured over calculated bearing capacity is defined as the bias λ_R :

$$\lambda_R = \frac{\text{measured bearing capacity}}{\text{calculated bearing capacity}} \quad (8)$$

This lump-sum procedure includes all sources of uncertainties related to the bearing capacity prediction such as scale effects, variation in soil properties, etc.

The statistics of the bias, especially its mean value and its coefficient of variation (COV), were used to analyze the model uncertainties.

5.2 Uncertainties in the bearing capacity of footings subjected to vertical-centric loading

Figure 4 summarizes the results of the statistical analysis for the vertical-centric loading cases. The overall mean bias was 1.59 for all 173 cases which indicates a systematic bearing capacity underprediction. The mean bias for footings in controlled soil conditions was 1.64 and higher, with a COV of 0.267, and therefore significantly different than that for footings in natural soil conditions (mean bias = 1.00, COV = 0.329).

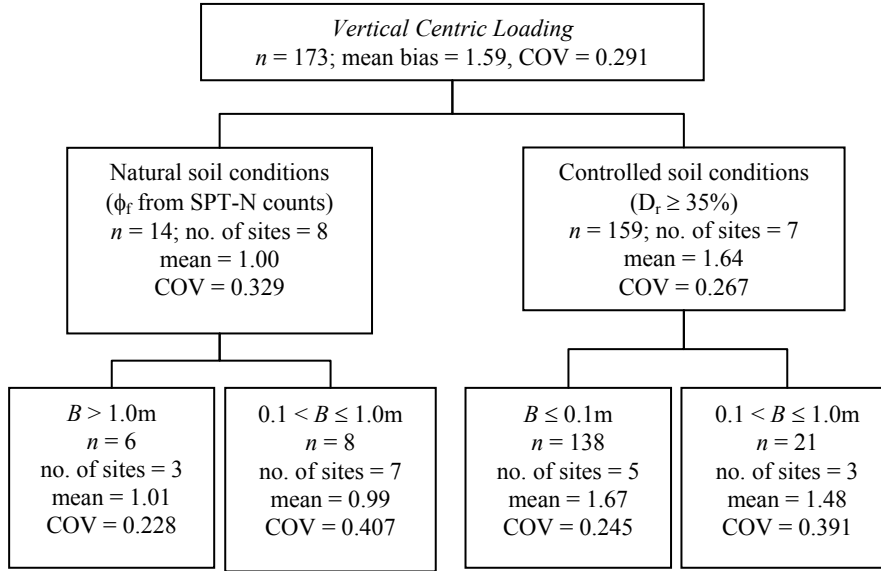


Figure 4. Summary of the bias for vertical-centric loading cases

The higher mean bias in controlled soil conditions is attributed to the conservatism in the theoretical prediction of the bearing capacity formulation as outlined in section 3.1. This conservatism especially results from the bearing capacity factor N_γ proposed by Vesic (1973) (see Table 3).

The uncertainty related to N_γ has been analyzed on the basis of load tests carried out on the surface of granular soils. Under such conditions, the bearing capacity only depends on the weight of the soil as the embedment and cohesion term in Eq. (2) are equal zero.

N_γ can, therefore, be back-calculated from the load tests and the obtained values can be related to the theoretical value proposed by Vesic (1973). With that the bias of the bearing capacity factor N_γ is defined as:

$$\lambda_{N_\gamma} = \frac{N_{\gamma\text{Exp}}}{N_{\gamma\text{Vesic}}} = \frac{q_u / (0.5 \cdot \gamma \cdot B \cdot s_\gamma)}{2 \cdot (N_q + 1) \cdot \tan \phi_f} \quad (9)$$

Figure 5 presents the bias λ_{N_γ} as a function of the soil friction angle ϕ_f . A clear trend of the bias increasing beyond 1.0 for friction angles $\phi_f \geq 42.5^\circ$ can be observed in Figure 5.

The best fit line of the bias λ_{N_γ} in Figure 5 is expressed as:

$$N_{\gamma\text{Exp}} = \exp(0.205 \cdot \phi_f - 8.655) \cdot N_{\gamma\text{Vesic}} \quad \text{for } 42.5^\circ \leq \phi_f \leq 46^\circ \quad (10)$$

with a coefficient of determination of $R^2 = 0.351$ indicating a large scatter.

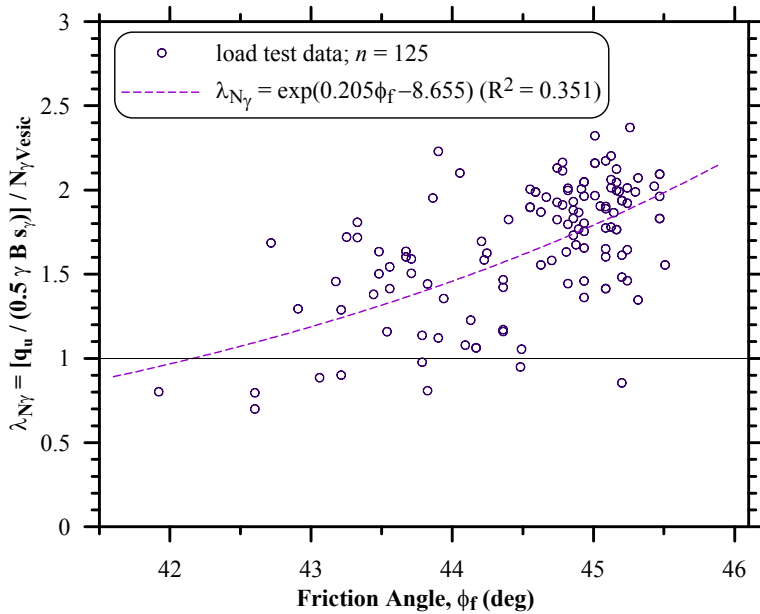


Figure 5. Bias of the bearing capacity factor N_γ as a function of the soil's friction angle ϕ_f

Figure 6 shows the bias of the calculated bearing capacity λ_R and the bias of the bearing capacity factor λ_{N_γ} for the considered range of soil friction angle. The overlapping biases suggest that the bias in the bearing capacity factor N_γ is the dominant factor affecting the uncertainty in the bearing capacity prediction whereas the shape factor has only a negligible influence considering that most foundations were of limited L/B ratio. This has been confirmed by the analysis of footings under vertical-eccentric, inclined-centric and inclined-eccentric loading which revealed a similar trend although the biases did not overlap as cases involving eccentric and/or inclined loading are also sensitive to the loading conditions and their effect on the bearing capacity.

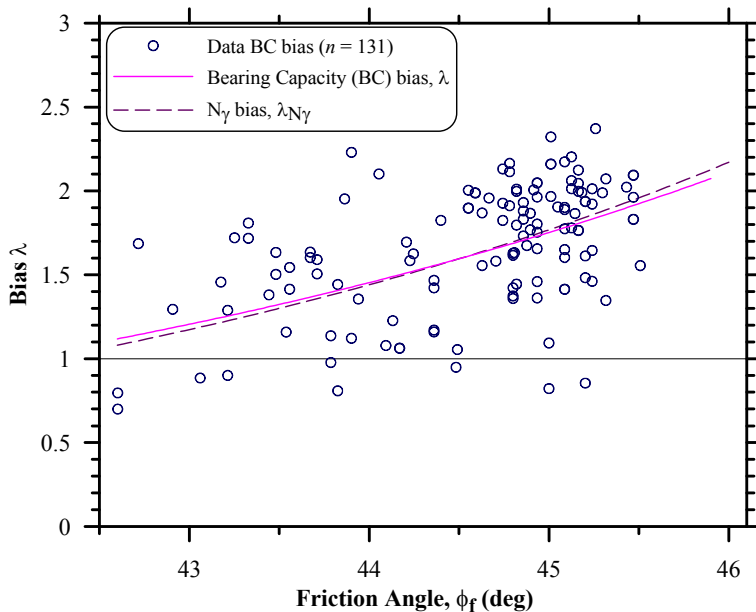


Figure 6. Bias of the bearing capacity prediction compared to the bias of the bearing capacity factor N_γ as a function of the friction angle for footings under vertical-centric loading

5.3 Uncertainties in the bearing capacity of footings subjected to combined loading

The uncertainty analysis for footings subjected to combined loading, i.e. vertical-eccentric, inclined-centric and inclined-eccentric loading, was based on results from small scale model tests under controlled laboratory conditions performed by DEGEBO (see e.g. summary in Weiß, 1978), Gottardi (1992), Montrasio (1994) and Perau (1995).

The uncertainty of the bearing capacity prediction for footings subjected to vertical-eccentric loading was based on the results from load tests with a radial load path, i.e. where a constant ratio $e = M/V$ was maintained during the test as the vertical load was applied at a constant eccentricity. A total number of 43 tests were examined. The resulting histogram and PDF of the bias as well as the relationship between measured and calculated bearing capacities are presented in Figure 7.

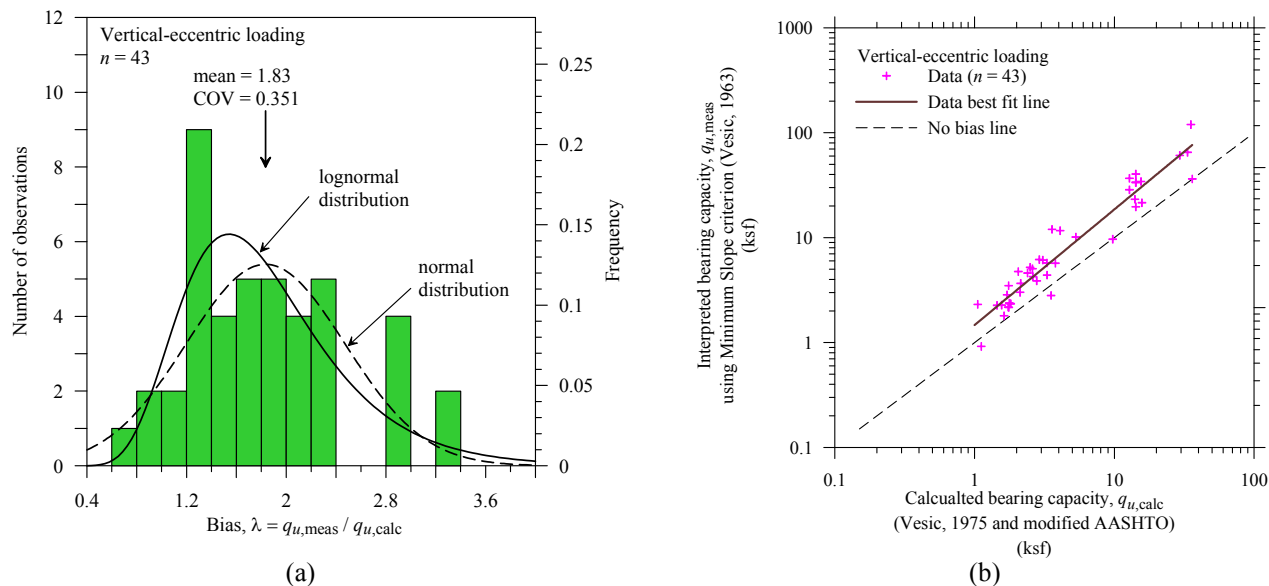


Figure 7. Histogram and probability density function of the bias (a) and relationship between measured and calculated bearing capacity (b) for all footings subjected to vertical-eccentric loading

The analysis shows a mean bias of 1.83 and a COV of 0.351 for all load tests. However, the DEGEBO tests conducted on larger footings ($0.5 \text{ m} \leq B \leq 1.0 \text{ m}$) lead to a significantly larger bias of 2.22 than the small scale model tests with $0.05 \text{ m} \leq B \leq 0.5 \text{ m}$ and a mean bias between 1.43 and 1.71 indicating a dependency of the bias on the footing size.

The available tests on foundations subjected to inclined-centric loading were either conducted with a radial load path (DEGEBO; Gottardi, 1992; Montrasio, 1994) or a step-like load path (Gottardi, 1992; Pe-rau, 1995). In the latter, the vertical load was increased to a certain value and then kept constant while the horizontal load was increased to failure. The difference in the applied load path did not have an influence on the bias statistics. As can be seen in Figure 8, a mean bias of 1.43 for all 39 tests was determined with a COV of 0.295. For this load combination, the DEGEBO tests lead to biases of similar magnitude as the small scale model tests.

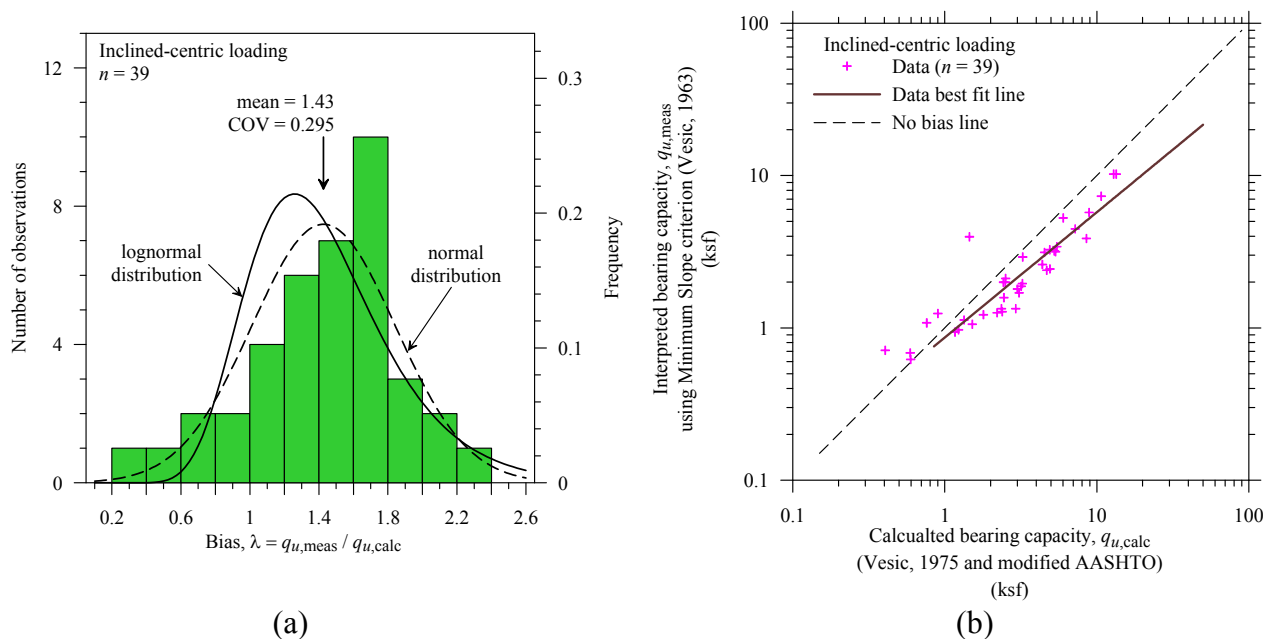


Figure 8. Histogram and probability density function of the bias (a) and relationship between measured and calculated bearing capacity (b) for all footings subjected to inclined-centric loading

Figure 9 shows the histogram and PDF of the bias as well as the relationship between measured and calculated capacity for the 29 tests on foundations subjected to inclined-eccentric loading. These tests were conducted with a radial or a step-like load path. Significant differences in the results due to the different load paths could not be identified in this case as well.

A mean bias of 2.43 with a COV of 0.508 was calculated for all tests. However, detailed examination revealed that the direction of the applied moment or load eccentricity in relation to the direction of the horizontal load affects the measured failure loads.

A resultant moment, which acts in the opposite direction to the horizontal load and causes a negative eccentricity (see Figure 10 top), induces rotations which counteract the horizontal displacements by the horizontal load. The resulting resistance, i.e. the failure load, is higher as compared to inclined-centric loading. A moment which acts in the same direction as the horizontal load and causes a positive eccentricity (see Figure 10 bottom) induces rotations which enforce the horizontal displacements, and hence, the resulting failure load is smaller as compared to inclined-centric loading.

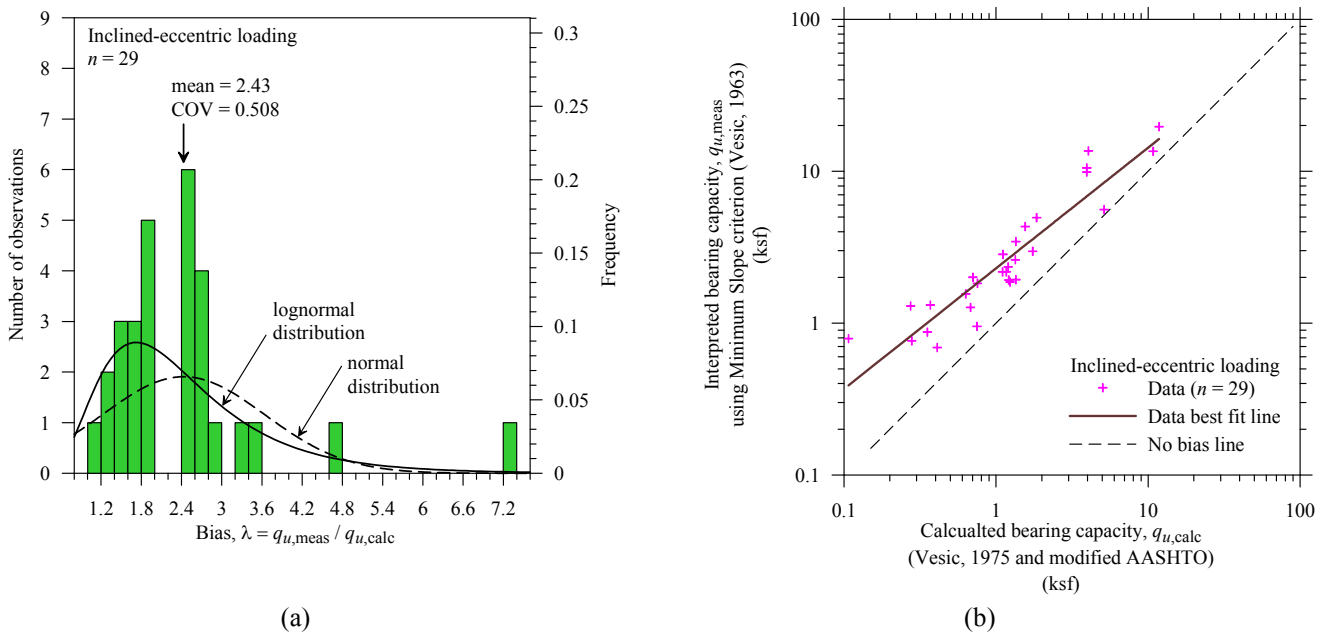
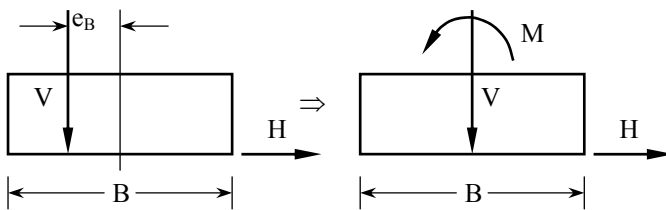
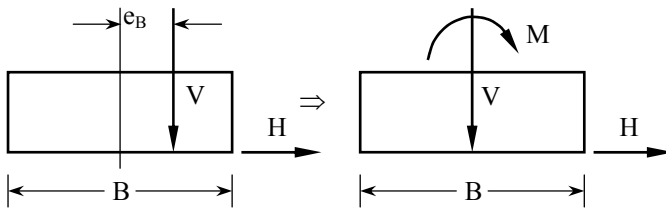


Figure 9. Histogram and probability density function of the bias (a) and relationship between measured and calculated bearing capacity (b) for all footings subjected to inclined-eccentric loading



Moment acting in direction opposite to the lateral loading – negative eccentricity



Moment acting in the same direction as the lateral loading – positive eccentricity

Figure 10. Loading directions for the case of inclined-eccentric loadings

Figures 11 and 12 show a significant difference in the bias when the different loading directions are considered. For cases with a negative eccentricity the mean bias is 3.43 compared to a mean bias of 2.16 for the cases with positive eccentricity. The results suggest that the loading direction needs to be considered in the evaluation of the resistance factors. It should, however, be noticed that the effect is less pronounced when the vertical load is relatively high, i.e. the load inclination is relatively small. Lesny (2001) demonstrated that for a vertical load level equal or greater than 0.3 the effect of the loading direction is negligible. The vertical load level is defined as the ratio of the vertical load to the vertical failure load under vertical-centric loading. While the findings clearly demonstrate an important physical effect, the practical ramification of this finding is yet to be investigated.

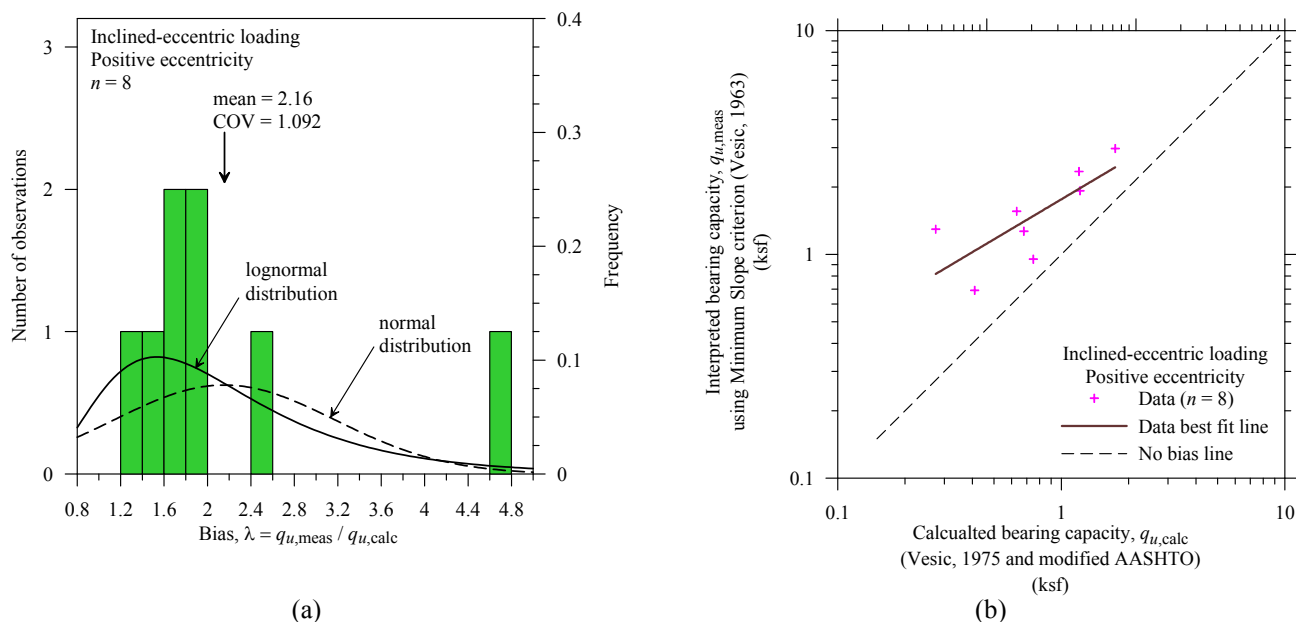


Figure 11. Histogram and probability density function of the bias (a) and relationship between measured and calculated bearing capacity (b) for footings subjected to inclined-eccentric loading with a positive eccentricity

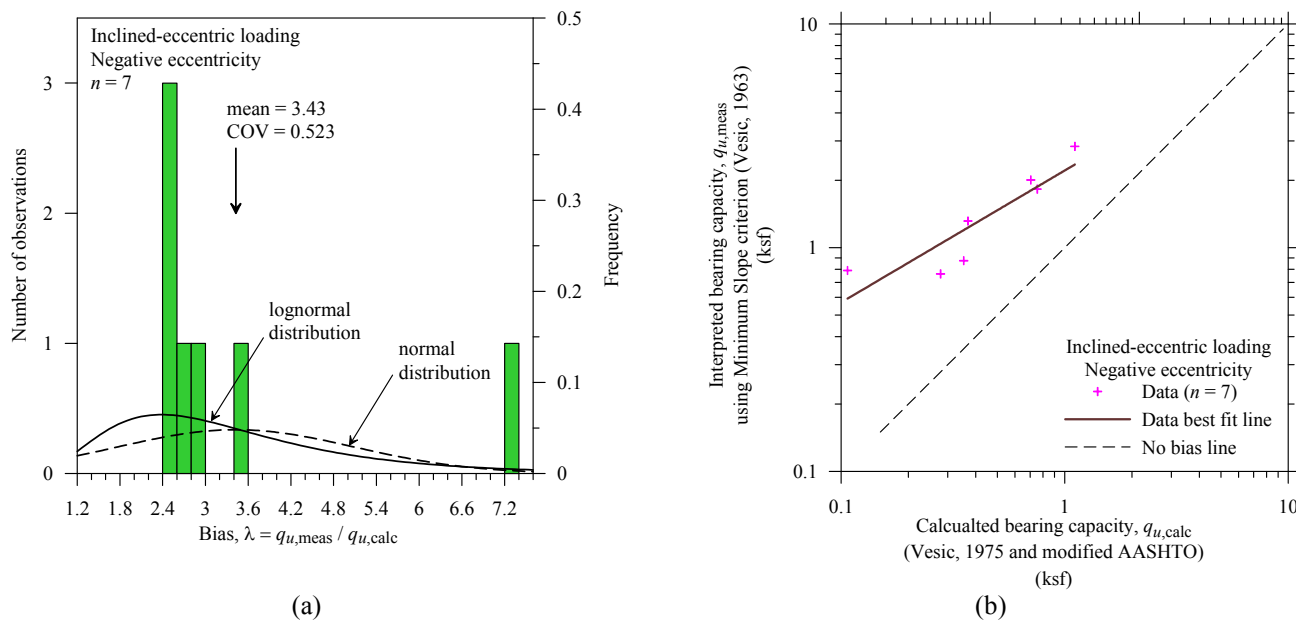


Figure 12. Histogram and probability density function of the bias (a) and relationship between measured and calculated bearing capacity (b) for all footings subjected to inclined-eccentric loading with a negative eccentricity

6 DERIVATION OF RESISTANCE FACTORS

6.1 Probabilistic analysis procedures

The partial factors used in the LRFD are derived in this research using so-called Level 2 approaches in which the uncertainties of the design variables are expressed by their mean, standard deviation and/or coefficient of variation. The limit state of the foundation is evaluated by using the First Order Second Moment (FOSM) method as an approximate iterative procedure as well as the more accurate Monte Carlo Simulation (MCS) procedure.

According to the FOSM as originally proposed by Cornell (1969) the mean and the variance of a limit state function $g(\bullet)$ are defined as:

$$\text{mean:} \quad m_g \approx g(m_1, m_2, m_3, \dots, m_n) \quad (11a)$$

$$\text{variance:} \quad \sigma_g^2 \approx \sum_{i=1}^n \left(\frac{\partial g}{\partial x_i} \right)^2 \cdot \sigma_i^2 \quad (11b)$$

In Eq. (11) m_i and σ_i are the means and the standard deviations of the basic variables (design parameters) x_i .

The FOSM was later used by Barker et al. (1991) to develop closed form solutions for the calibration of geotechnical resistance factors ϕ that appear in previous AASHTO LRFD specifications:

$$\phi = \frac{\lambda_R \left(\sum \gamma_i \cdot Q_i \right) \cdot \sqrt{\frac{1 + \text{COV}_Q^2}{1 + \text{COV}_R^2}}}{m_Q \cdot \exp \left\{ \beta \cdot \sqrt{\ln \left[(1 + \text{COV}_R^2) \cdot (1 + \text{COV}_Q^2) \right]} \right\}} \quad (12)$$

In Eq. (12) Q_i are the loads, λ_R is the resistance bias factor defined as the mean ratio of measured resistance over calculated resistance, m_Q is the mean of the loads, COV_R and COV_Q are the coefficients of variation of the resistance and the load, respectively, γ_i are the load factors and β is the target reliability index.

The approach adopted in this research differs from the original Level 2 approach as the load factors and related uncertainties used in the analysis are previously selected (see section 2) and then utilized to determine the resistance factors for a given target reliability index and a given range of loads.

MCS involves the numerical integration of the failure probability defined as:

$$p_f = P(g \leq 0) = \frac{1}{N} \cdot \sum_{i=1}^n I[g \leq 0] \quad (13)$$

In Eq. (13) I is an indicator function which is equal to 1 for $g_i \leq 0$, i.e., when the resulting limit state is exceeded (failure), and equal to 0 for $g_i > 0$ when the limit state is not exceeded. N is the number of simulations carried out.

In order to evaluate equation (13) the basic variables and their distributions first need to be defined. Then N random samples for each design variable based on their distributions, i.e. using the statistics of loads and resistances, are generated. The limit state function is evaluated N times taking a set of the design values previously generated and the number N_f is counted for which the indicator function is equal to 1, i.e. failure occurred. The failure probability is finally obtained as the ratio N_f/N .

The resistance factor based on the MCS can be calculated using the fact that to attain a target failure probability p_{fT} , the limit state must be exceeded N_{fT} times. As in the current LRFD concept only one resistance factor needs to be determined for one limit state, while keeping the load factors constant, a suitable choice of the resistance factor shifts the limit state function so that failure occurs N_{fT} times.

It has to be noticed that the results of a MCS is only as good as the determination of the distributions of loads and resistance. This means, the statistical parameters need to be defined as good as possible.

6.2 Definition of the target reliability index

Instead of the failure probability, the safety of a system often is expressed by the reliability index β which describes the margin of safety by the number of standard deviations of the probability density function for the limit state g , separating the mean of g from the failure zone beginning at $g = 0$. The reliability index is related to the failure probability by the error function Φ as given in Eq. (14).

$$p_f = \Phi(-\beta) \quad (14)$$

Accordingly, the target reliability index is the safety margin to be implemented in the design. It can be derived either from the reliability levels implicit in the current WSD codes or by a cost-benefit analysis with an optimum reliability based on minimum costs including costs of economic losses and consequences due to failure. The latter is a difficult process as especially costs related to human injuries or loss of life are hard to determine and therefore not adopted in this research.

Using a target reliability derived from WSD represents the acceptable risks in the current design practice and may therefore be an adequate starting point for a code revision. However, such reliability levels can have considerable variations as various studies have shown (e.g. Phoon and Kulhawy, 2000; Honjo and Amatya, 2005).

It seems to be logical and convenient, therefore, to assign a target reliability index for the foundations equal to that assigned for the superstructure to maintain a comparable reliability level, although the actual reliability level of the combined system of super- and substructure remains unknown. For foundations in/on granular soils a target reliability index of $\beta_T = 3$ has been selected in the probabilistic analyses.

7 RECOMMENDED RESISTANCE FACTORS

7.1 General

The aforementioned investigations of the bearing capacity equation vs. shallow foundations load test databases lead to the conclusion that one single resistance factor for the bearing capacity is not sufficient to address the different loading conditions leading to different levels of uncertainties. Consequently, different resistance factors were established based on the probabilistic analyses, each for vertical-centric, vertical-eccentric, inclined-centric and inclined-eccentric loading conditions. These resistance factors are valid only with the calculation methods specified previously for the respective resistances.

7.2 Vertical-centric loading

For vertical-centric loading the bias change with the soil's friction angle as described in section 5.2 had to be considered in developing the resistance factors. For this, subsets of the database based on the magnitude of ϕ_f were analyzed for possible outliers to improve the quality of the database and to achieve a better fit of the assumed probability distribution. In the end, only one outlier had been removed, so that 172 cases were available for the resistance factor calibration. Further on, a lognormal distribution of the bias has been defined for the whole range of ϕ_f .

The MCS calculations are based on a mean bias of:

$$\lambda_{BC} = 0.398 \exp(0.0372 \cdot \phi_f) \quad (15)$$

with a COV_λ of 0.25 for controlled soil conditions and 0.35 for natural soil conditions. From the results of the calculations the resistance factors presented in Table 8 finally have been recommended specified for natural soil conditions and controlled soil conditions. The values are valid for soils with a relative density of 35% and greater.

For loose soils with a smaller relative density and friction angles less than 30° it is recommended to consider either ground improvement or ground replacement in the zone of influence beneath the footing or to choose an alternative foundation.

Table 8. Recommended resistance factors for vertical-centric loading

Soil friction angle [°]	Recommended resistance factor ϕ ($\beta_T = 3$)	
	natural soil conditions	controlled soil conditions
30 – 34	0.40	0.50
35 – 36	0.45	0.60
37 – 39	0.50	0.70
40 – 44	0.55	0.75
≥ 45	0.65	0.80

7.3 Vertical-eccentric loading

Analysis of the cases under vertical-eccentric loading revealed that a clear unique correlation between the bearing capacity bias and the soil’s friction angle as in case of vertical-centric loading does not exist (see Figure 13). Derivation of resistance factors depending on the soil friction angle assuming a lognormal distribution of the bias lead to values around 1.0 and are far greater than the values presented in Table 8. This is not consistent as the uncertainties involved with vertical-eccentric loading should not be less than those with vertical-centric loading. Further analysis indicated that the footing size affects the bearing capacity bias, too, but with the available data it was not possible to isolate the effects of the footing size from the effect of the soil friction angle. Thus, it seems to be justified and appropriate to extend the dataset for vertical-eccentric loading by the dataset for vertical-centric loading for deriving the resistance factors because (i) when the source of the lateral load is not permanent, the foundation supports vertical-centric loading in some situations, and (ii) very often the magnitude of the lateral load and with that the eccentricity is not known in the design phase of the bridge foundation.

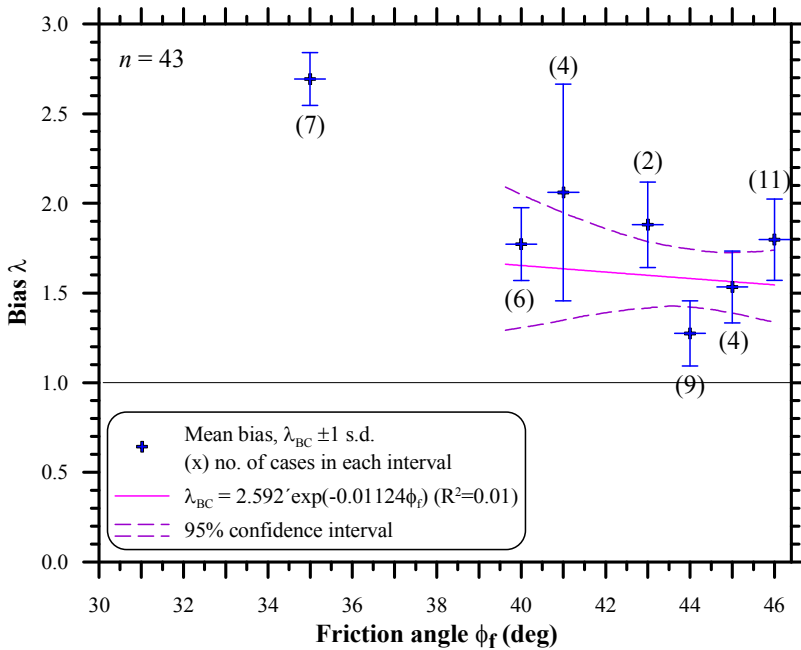


Figure 13. Bias of the bearing capacity prediction versus soil friction angle for footings under vertical-eccentric loading (seven cases for $\phi_f = 35^\circ$ have been ignored as outliers for obtaining the best fit line)

As a result of the above, the same resistance factors used for vertical-centric loading and presented in Table 8 are recommended for vertical-eccentric loading, too. These are verified by resistance factors obtained on the basis of Figure 13 with a constant mean bias of 1.60 for friction angles between 40° and 46° and a COV for natural and controlled soil conditions of 0.35 and 0.30, respectively:

- Natural soil conditions, for all ϕ_f : $\phi = 0.65$ (from MCS: $\phi = 0.687$)
- Controlled soil conditions, for all ϕ_f : $\phi = 0.75$ (from MCS: $\phi = 0.796$)

7.4 Inclined-centric loading

For footings under inclined-centric loading no clear trend of the bias associated to the load inclination and the orientation of the horizontal load or the footing size exists. Thus, the resistance factors again have been obtained based on the variation of the bearing capacity bias on the soil friction angle:

$$\lambda_{BC} = 1.25 + 0.0041 \cdot \phi_f \quad (16)$$

Eq. (16) has been derived as a best-fit line from an evaluation of the bearing capacity bias versus the soil friction angle. A COV of 0.35 has been adopted for controlled soil conditions and a COV of 0.40 for natural soil conditions. The resistance factors resulting from the MCS calculations needed to be adjusted to guarantee a safe design. Table 9 summarizes the finally recommended resistance factors.

Table 9. Recommended resistance factors for inclined-centric loading

Soil friction angle [°]	Recommended resistance factor ϕ ($\beta_T = 3$)	
	natural soil conditions	controlled soil conditions
30 – 34	0.40	0.40
35 – 36	0.40	0.40
37 – 39	0.40	0.45
40 – 44	0.45	0.50
≥ 45	0.50	0.55

7.5 Inclined-eccentric loading

Due to the limited available datasets resistance factors for inclined-eccentric loading can only be given as guidance. For a positive loading eccentricity as indicated in Figure 10 (bottom) the probabilistic analysis results in a resistance factor of $\phi = 0.55$ for all eight investigated cases with $44.5^\circ \leq \phi_f \leq 45^\circ$. For a negative loading eccentricity according to Figure 10 (top) the analysis lead to a resistance factor of $\phi = 0.85$ for all seven cases with $44.5^\circ \leq \phi_f \leq 45^\circ$. On this basis the resistance factors presented in Table 10 are recommended.

Table 10. Recommended resistance factors for inclined-eccentric loading

Soil friction angle [°]	Recommended resistance factor ϕ ($\beta_T = 3$)			
	natural soil conditions		controlled soil conditions	
	positive	negative	positive	negative
30 – 34	0.35	0.65	0.40	0.70
35 – 36	0.35	0.70	0.40	0.70
37 – 39	0.40	0.70	0.45	0.75
40 – 44	0.40	0.75	0.50	0.80
≥ 45	0.45	0.75	0.50	0.80

8 CONCLUSIONS

The resistance factors recommended in this research are soundly based on the quantified uncertainties of the design methods and follow the parameters that control them. These parameters present a radical change to the existing design specifications for bridge foundations as the bearing capacity of shallow foundations on granular soils is calibrated according to the soil placement (natural vs. controlled conditions) and the magnitude of the angle of internal friction. Further, all possible loading conditions were calibrated, namely vertical-centric, vertical-eccentric, inclined-centric and inclined-eccentric.

The implementation of the developed LRFD procedure is expected to provide a safe design of shallow foundations with a consistent level of reliability for the different design conditions.

The application of these findings in the design of shallow foundations needs, however, to be implemented in the context of a total design including all limit states, especially the serviceability limit state.

ACKNOWLEDGEMENTS

The material presented in this paper is based on a research supported by the National Cooperative Highway Research Program (NCHRP) project 24-31 under a contract with Geosciences Testing and Research Inc. (GTR). NCHRP Report 651 provides a summary of the study. The participants and contributors in this research are greatly acknowledged, specifically Dr. Shailendra Amatya and Mr. Robert Muganga working at the UML Geotechnical Engineering Research Laboratory, Dr. Aloys Kisse working at the University of Duisburg – Essen, and Ms. Mary Canniff of Geosciences Testing and Research. Also are acknowledged Ms. Yu Fu and Mr. Jenia Nemirovsky who participated in the initial establishment of UML-GTR ShalFound07 database working at the Geotechnical Engineering Research Laboratory of the University of Massachusetts Lowell.

REFERENCES

- AASHTO 2007. LRFD Bridge Design Specifications Section 10: Foundations, American Association of State Highway & Transportation Officials, Washington, DC.
- AASHTO 2008. LRFD Bridge Design Specifications Section 10: Foundations, American Association of State Highway & Transportation Officials, Washington, DC.
- Brinch Hansen, J. 1970. A Revised and Extend Formula for Bearing Capacity, Akademiet for de Tekniske Videnskaber, Geoteknisk Institut, Bullentin No.28, Copenhagen, pp.5-11.
- De Beer, E.E. 1967 Proefondervindelijke bijdrage tot de studie van het gransdragvermogen van zand onder funderingen op staal; Bepaling von der vormfactor sb, Annales des Travaux Publics de Belgique, 68, No.6, pp.481-506; 69, No.1, pp.41-88; No.4, pp.321-360; No.5, pp.395-442; No.6, pp.495-522.
- DIN EN 1997-1 2009. Entwurf, Berechnung und Bemessung in der Geotechnik – Teil 1: Allgemeine Regeln. , German version of EN 1997-1:2004. Normenausschuss Bauwesen im Deutschen Institut für Normung. Beuth Verlag, Berlin.
- Gottardi, G. 1992. Modellazione del comportamento di fondazioni superficiali su sabbia soggette a diverse condizioni di carico, Dottorato di ricerca in ingegneria geotecnica, Istituto di Costruzioni Marittime e di Geotecnica, Università di Padova
- Nowak, A. 1999. NCHRP Report 368: Calibration of LRFD Bridge Design Code. National Cooperative Highway Research Program, TRB, Washington, DC.
- Kimmerling, R.E. 2002. Geotechnical Engineering Circular No. 6 Shallow Foundations, FHWA Report no. FHWA-IF-02-054, Washington, DC, 310pp.
- Kulhawy, F. and Mayne, P. 1990. Manual on Estimation of Soil Properties for Foundation Design, Report EPRI-EL-6800, Electric Power Research Institute, Palo Alto, CA
- Lesny, K. 2001. Entwicklung eines konsistenten Versagensmodells zum Nachweis der Standsicherheit flachgegründeter Fundamente. Mitteilungen aus dem Fachgebiet Grundbau und Bodenmechanik der Universität Essen, Heft 27, Hrsg.: Prof. Dr.-Ing. W. Richwien, Verlag Glueckauf, Essen, in German.
- Montrasio, L. 1994. Un Metodo per il calcolo die cedimenti di fondazioni su sabbia soggette a carichi eccentrici e inclinati, Dottorato di ricerca in Ingegneria Geotecnica, Università di Milano (in Italian).
- NAVFAC. 1986. Foundation and Earth Structures, Design Manual DM7.02, Naval Facilities Engineering Command, Alexandria, Virginia
- Paikowsky, S.G. with contributions by Birgission G., McVay M., Nguyen T., Kuo C., Baecher G., Ayyub B., Stenerson K., O'Mally K., Chernauskas L., and O'Neill M. 2004. NCHRP Report 507 Load and Resistance Factor Design (LRFD) for Deep Foundations, National Cooperative Highway Research Program report for Project NCHRP 24-17, TRB, Washington, DC, 2004, pp. 134 (not including Appendices), http://onlinepubs.trb.org/onlinepubs/nchrp/nchrp_rpt_507.pdf
- Paikowsky, S.G., Lesny, K., Amatya, S., Kisse, A., Muganga, R. and Canniff, M. 2010. NCHRP Report 651 LRFD Design and Construction of Shallow Foundations for Highway Bridge Structures, National Cooperative Highway Research Program Report for Project NCHRP 24-31, TRB, Washington, DC, June 2010, pp. 139 excluding appendices. http://onlinepubs.trb.org/onlinepubs/nchrp/nchrp_rpt_651.pdf
- Paikowsky, S.G., Player, C.M. and Connors, P.J. 1995. A dual interface apparatus for testing unrestricted friction of soil along solid surfaces, Geotechnical Testing Journals, GTJODJ, Vol.18(2), pp.168-193
- Perau, E. 1995. Ein systematischer Ansatz zur Berechnung des Grundbruchwiderstands von Fundamenten. Mitteilungen aus dem Fachgebiet Grundbau und Bodenmechanik der Universität Essen, Heft 19, Hrsg.: Prof. Dr.-Ing. W. Richwien, Essen: Glückauf-Verlag
- Prandtl, L. 1921. Ueber die Eindringfestigkeit (Haerte) plastischer Baustoffe und die Festigkeit von Schneiden. Zeitschrift für angewandte Mathematik und Mechanik 1, Band 1, pp.15-20.
- Reissner, H. 1924. Zum Erddruckproblem, Proc., 1st Int. Congress of Applied Mechanics, Delft, pp.295-311.
- Teixeira, A., Gomes Correia, A., Honjo, Y., and Henriques, A. 2011. Reliability analysis of a pile foundation in a residual soil: contribution of the uncertainties involved and partial factors, to be published in the 3rd Intl. Symposium on Geotechnical Safety and Risk (ISGSR2011), 2-3, June, Munich, Germany.
- Vesić, A. 1963 Bearing capacity of deep foundations in sand, Highway Research Record, 39, National Academy of Sciences, National Research Council, pp.112-153

- Vesić, A. 1975. Bearing Capacity of Shallow Foundations, Foundation Engineering Handbook (eds. H.F. Winterkorn and H.Y. Fang), Van Nostrand Reinhold, New York, pp.121-147.
- Weiß, K. 1978. 50 Jahre Deutsche Forschungsgesellschaft für Bodenmechanik (Degebo). Mitteilungen der Deutschen Forschungsgesellschaft für Bodenmechanik (Degebo) an der Technischen Universität Berlin, Heft 33.